

ORIGINAL RESEARCH

Role of diffusion weighted imaging in evaluation of the Intracerebral hemorrhage

Dr. Sandeep Kaur Toor

Consultant Radiologist, Radiodiagnosis, Telrad, India

Corresponding Author

Dr. Sandeep Kaur Toor

Consultant Radiologist, Radiodiagnosis, Telrad, India

Email: drssandhoo@gmail.com

Received: 11 February, 2023

Accepted: 16 March, 2023

ABSTRACT

The application of strong magnetic field gradients during proton MR imaging allows one to observe differences in molecular self-diffusion [6]. The basis for this diffusion is molecular translational (Brownian) motion, which leads to attenuation of signal intensity in each image voxel. Proton diffusion rates differ according to the tissue type; and specific techniques, such as intravoxel incoherent motion (IVIM) imaging, resulting in an apparent diffusion coefficient (ADC) image, have been developed to exploit these differences (6). The generalized model for the appearance of ICH on MR images attributes the various signal intensity patterns of evolving ICH to the oxygenation state of hemoglobin and the integrity of the red blood cells (13,14).

This is an open access journal, and articles are distributed under the terms of the Creative Commons Attribution-Non Commercial-Share Alike 4.0 License, which allows others to remix, tweak, and build upon the work non-commercially, as long as appropriate credit is given and the new creations are licensed under the identical terms.

INTRODUCTION

The usual pattern of magnetic resonance (MR) appearances corresponding to the different stages of intracerebral hemorrhage (ICH) is well known. The generalized model for the appearance of ICH on MR images attributes the various signal intensity patterns of evolving ICH to the oxygenation state of hemoglobin and the integrity of the red blood cells (43,44).

CT (Computerized Tomography) and MRI are used effectively for the detection of intracranial hematomas. Non-contrast computed tomography (CT) has been the standard imaging modality for the initial evaluation of patients presenting with acute stroke symptoms (1,2). The primary diagnostic advantage of CT in the hyperacute phase (0–6 h) is its ability to rule out the presence of hemorrhage. Accurate early detection of blood is crucial since a history of intracerebral hemorrhage is a contraindication to the use of thrombolytic agents. However, a major disadvantage of conventional CT within the first few hours of symptom onset is its limited sensitivity for identifying early evidence of cerebral ischemia (7).

MRI findings of different stages of hematomas are well established. MR signal intensity resulting from blood is mainly affected by several complicated factors such as hematocrit, oxygen content, tissue Ph, protein content of the clot, membrane stability of red blood cells, types of hemoglobin and chemical status of the iron that hemoglobin contains. In addition to

conventional MRI sequences, DWI has become an important imaging modality for detecting the stages of intracerebral hematomas. Several studies assessed the apparent diffusion coefficient (ADC) values of intracerebral hematomas according to their stages and reported that they have similar ADC values (8-12)

MR diffusion weighted imaging (DWI) uses the signal loss associated with the random thermal motion of water molecules in the presence of magnetic field gradients to derive a parameter (the so-called apparent diffusion coefficient) that directly reflects the translational mobility of the water molecules in the tissues. Applications of this technique in the context of neuro-vascular imaging include the early detection and assessment of stroke, tumor characterisation, evaluation of multiple sclerosis. (2) The generalized model for the appearance of ICH on MR images attributes the various signal intensity patterns of evolving ICH to the oxygenation state of hemoglobin and the integrity of the red blood cells (4,5)

MATERIALS AND METHODS

PURPOSE

To correlate the findings of MRI diffusion weighted imaging along with the T1WI, T2WI and T2 FLAIR findings in cases of intracerebral lobar bleed.

PATIENTS

This was a retrospective study of MR examinations performed in 40 patients [aged 41-90 (mean age 65.2)

years] with spontaneous intracerebral hematoma unrelated to neoplasm, infarction, trauma or coagulopathy. The details including the name, gender and age of the patient were obliterated from the data.

PROCEDURE

MR examination was done for all patients using 1.5 T machine. The conventional MR imaging protocol included (a) axial T1-weighted spin-echo ; (b) axial T2-weighted fast spin-echo; and (c) axial FLAIR .

Singleshot, spin-echo, echo-planar DWI sequences were obtained by applying diffusion gradients in three orthogonal directions at each slice, with two diffusion weightings (b value = 0 and 900 or 1000 s/mm²).

INTERPRETATION

The signal intensity changes of hematomas were determined by visual analysis of T2WI, T1WI , T2 FLAIR images;ADC maps and trace DWI (b=1000 sec/mm²) and also compared with normal white matter of contralateral cerebral hemispheres.

Diffusion weighted imaging was analyzed for- stage of hemorrhage; According to the time interval between symptom onset and initial MRI, four stages were categorized: hyperacute, acute, early subacute and late subacute.

For the determination of signal characteristic differences and expression of their contribution to the diagnosis, different phases of groups were compared with each other. For the assesment of detectability of intracranial hematomas on DWI, conventional MRI

sequences were accepted as a gold standard for intracerebral hematomas.

RESULTS

All intracerebral hematomas detected on conventional MRI sequences were also detected on DWI.

Five cases of hyperacute intracerebral hematomas were evaluated - the MRI was done within 6 hours of presentation hyperintense on DWI and hypointense on ADC maps . The lesion was hypointense to isointense on T1WI and isointense to hyperintense on T2WI/ T2 FLAIR images.

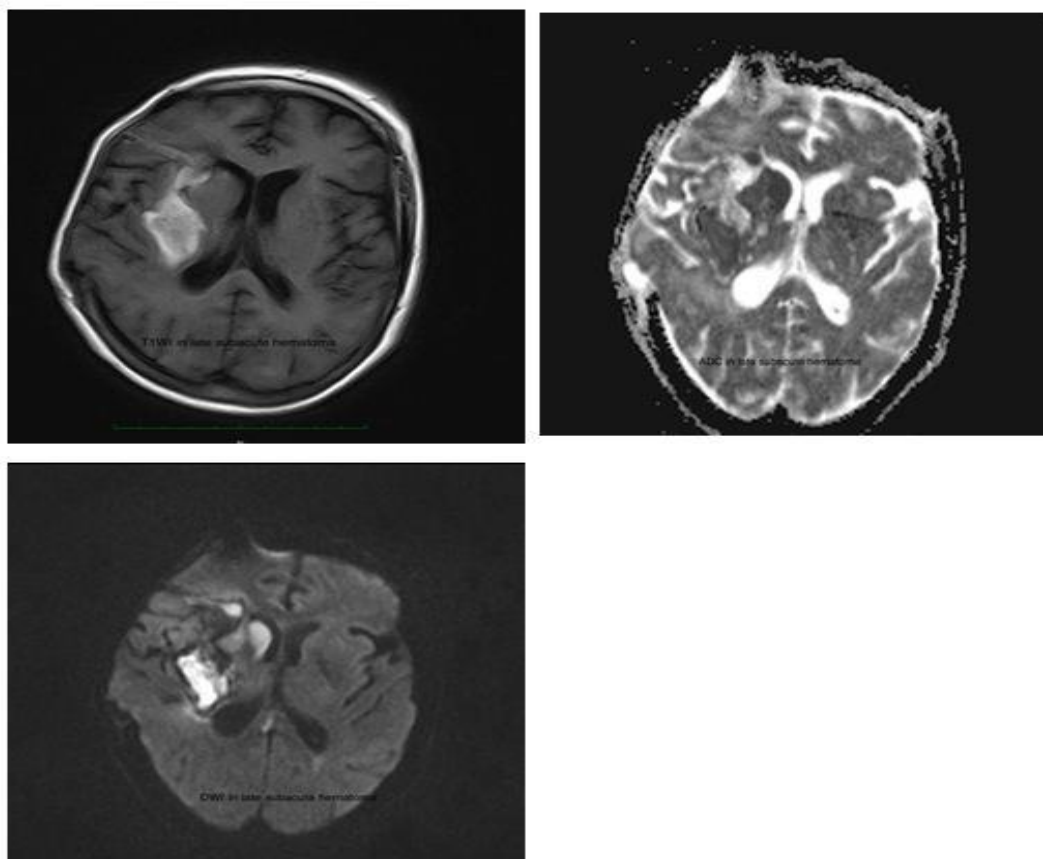
Five case of acute intracerebral hematomas(between 6 hours- 3 days) were evaluated , based on the time of presentation since onset of symptoms. They were hypointense on both T1WI and T2WI; both ADC and DWI images.

Ten case of early subacute intracerebral hematomas(3-7 days) were evaluated. These were hyperintense on T1WI, hypointense on T2WI;markedly hypointense on both DWI and ADC maps .

Ten cases of late subacute intracerebral hematomas(7-14 days) were heterogenously hyperintense on DWI and hypointense on ADC maps; and are hyperintense on both T1WI/T2WI.

Ten intracerebral chronic hematomas had a varied appearance from markedly hypointense appearance to hyperintense center with a hypointense peripheral rim on DWI. On ADC maps, most lesions were markedly hypointense on both DWI and ADC maps. These appear hypointense on both T1WI and T2WI.

Age of hematoma	T2WI	T1WI	DWI	ADC
Hyper acute (<6 hours)	Isointense to hyperintense	Isointense to hypointense	Hyperintense	Hypointense
Acute (6 hours-3 days)	Hypointense	Hypointense	Hypointense	Hypointense
Early subacute(3-7 days)	Hypointense	Hyperintense	Hypointense	Hypointense
Late subacute(7-14 days)	Hyperintense	Hyperintense	Hyperintense	Hypointense
Chronic (>14days)	Hyperintense centre with hypointense rim	Hypointense	Hypointense or hyperintense	Hypointense



DISCUSSION

Neuroimaging plays a crucial role in the evaluation of patients presenting with acute stroke symptoms. While patient symptoms and clinical examinations may suggest the diagnosis, only brain imaging studies can confirm the diagnosis and differentiate hemorrhage from ischemia with high accuracy. This differentiation is critical in making acute treatment decisions, including patient eligibility for thrombolytic therapy (15,16).

HYPER ACUTE HEMATOMAS

In this study all the five cases of hyperacute hematoma, were detected by DWI showing heterogeneous hyperintense core, hypointense rim surrounded by perifocal brain edema. The central hyperintensity has been attributed to intracellular oxyhemoglobin and the hypointense rim to early intracellular deoxyhemoglobin at the periphery of a hematoma. This characteristic hypointense rim has been reported to occur within the first few hours of hemorrhage and in patients with acute neurologic symptoms is valuable for differentiating between acute ischemic stroke and hemorrhage (16,17).

Hypointensity within a hyperacute hematoma, revealed by DWI, may be an important feature for differentiating hemorrhage from infarction in the practical clinical setting of hyperacute stroke. This focal hypointensity seen at DWI within a hyperacute hematoma may be caused by unclotted liquid separated from a retracted clot (19,20). Previous

studies suggested that the reason of hypointensity of hyperacute hematoma seen on T2 weighted images was early formation of deoxyhemoglobin which had magnetic susceptibility effect (23-25). Oxyhemoglobin is hyperintense on DWI. Its ADC values are lower than normal brain parenchyma. This suggests that restricted water diffusion are inside red blood cells. This hypointense rim was more obvious in GRE than in DWI in the current study. The signal intensity of hyperacute ICH observed at DWI was consistent with the findings of previous studies (18).

ACUTE HEMATOMA

In the current study, all the cases of acute hematoma and cases of early subacute hematoma were detected by DWI showing markedly hypointense core at DWI, T2-weighted images, FLAIR and GRE. This hypointensity has been attributed to the magnetic field inhomogeneity caused by paramagnetic intracellular deoxyhemoglobin in acute hematoma (26) and paramagnetic intracellular methemoglobin in early subacute hematoma (27). At both stages, DWI consistently revealed that in all these patients, a thin, markedly hyperintense rim, varying in thickness and completeness, was present at the periphery of the hematoma. The bright rims corresponded to the areas of hyperintensity seen on T2-weighted images. In Echo-planar gradient-echo images the signal intensities observed were markedly hypointense, though the hyperintense rim seen at DWI was not demonstrated. T1-weighted images showed the

hematoma as heterogeneously isointense at the acute stage and markedly hyperintense at the early subacute stage.

The most important two factors that cause these signal intensity patterns are identified as hemoglobin-oxygen status and accompanied presence of intact cells that compartmentalize paramagnetic material and paramagnetic iron. In addition they defined markedly hyperintense rims in all patients with hyperacute, acute, and subacute hematomas on DWI. Wiesmann et al. (28) suggested susceptibility artefacts as a probable cause of hyperintense rims surrounding acute or subacute hematomas. Although Kang et al. (29) reported that this hypointense rim formation was not a result of a susceptibility artefact caused by paramagnetic material such as intracellular deoxyhemoglobin or methemoglobin but may be due to vasogenic edema which leads to T2 shine-through effects.

LATE SUBACUTE INTRACEREBRAL HEMATOMA

At late subacute hematoma phase red blood cell lysis occurs and compartmentalization of methemoglobin disappears. Also intracellular contents spread to extracellular space leading increased viscosity. The other biological change in this phase is hypercellularity that is due to the infiltration of inflammatory cells and macrophages. All these changes can effect molecular diffusion of hematoma (31-33).

Ebisu et al. (30) and Kang et al. (29) showed that late subacute hematoma was hyperintense on DWI while it had a lower signal intensity than normal white matter on ADC maps. In this study all of the subacute hematomas were hyperintense on DWI and hypointense on ADC maps.

Late subacute hematoma in the current study, showed marked hyperintense core with hypo-intense rim. All the cases also showed marked hyper intensity at T1- and T2-weighted, and FLAIR images while GRE demonstrated heterogeneous hyperintensity (34,35).

CHRONIC INTRACEREBRAL HEMATOMA

After a while, methemoglobin resorbs or precipitates and signal intensity of hematoma on T1 weighted images decreases. Higher water content leads to elongated T1-T2 relaxation times. From the beginning of hemorrhage, hemoglobin is phagocytized continuously. Hemoglobin products ferritin and hemosiderin persists in phagocytic cells that are indicators of an old hemorrhage which is located at the periphery of hematoma (36,38).

Hemosiderin and ferritin cause magnetic susceptibility artefacts which are seen predominantly on T2 weighted images (36,37,38). Chronic hematomas are hyperintense on DWI (8,10). But older chronic hematomas may exhibit hypointense signal characteristics (39). Chronic hematomas are hyperintense on DWI (8,10). But older chronic

hematomas may exhibit hypointense signal characteristics (39). An accurate calculation on DWI is difficult because of the peripheral deposits of hemosiderin and ferritin (9,38)

CONCLUSION

Intracerebral hematomas are markedly hypointense on DWI because of magnetic susceptibility effects of hemosiderin, intracellular deoxyhemoglobin and methemoglobin. Thus all of acute and early subacute hematomas and some of the chronic hematomas have similar signal intensity characteristics on DWI.

A better understanding of the DWI findings of intracerebral hematoma can be helpful for the differentiation of intracerebral hematoma from acute infarction and for the further characterization of intracranial hemorrhagic lesions

BIBLIOGRAPHY

1. Carhuapoma JR, Wang P, Beauchamp NJ, Hanley DF, Barker PB. Diffusion- perfusion MR evaluation and spectroscopy before and after surgical therapy for intracerebral hemorrhage. *Neurocrit Care* 2005;2(1):23-7.
2. Adams Jr HP, Adams RJ, Brott T, et al. Guidelines for the early management of patients with ischemic stroke. *Stroke* 2003;34:1056-83.
3. R Luytjens, S Boujraf, S Sourbron, M Osteaux. Diffusion and perfusion MRI: basic physics, *European Journal of Radiology*, Volume 38, Issue 1, 2001.
4. Gomori JM, Grossman RI, Goldberg HI, Zimmerman RA, Bilaniuk LT. Intracranial hematomas: imaging by high-field MR. *Radiology* 1985;157:87-93 2.
5. Bradley WG. MR appearance of hemorrhage in the brain. *Radiology* 1993;189:15-26
6. Le Bihan D, Breton E, Lallemand D, Aubin M-L, Vignaud J, Laval-Jeanie!
7. M. Separation of diffusion and perfusion in intravoxel incoherent motion MR imaging. *Radiology* 1988;168:497-505.
8. Baird AE, Warach S. Magnetic resonance imaging of acute stroke. *J Cereb Blood Flow Metab* 1998;18:583-609.
9. Kang BK, Na DG, Ryoo JW, et al. Diffusion-weighted MR imaging of intracerebral hemorrhage. *Korean J Radiol* 2001; 2: 183-191.
10. Does MD, Zhong J, Gore JC. In vivo measurement of ADC change due to intravascular susceptibility variation. *Magn Reson Med* 1999; 41: 236-240.
11. González RG, Schaefer PW, Buonanno FS, et al. Diffusion-weighted MR imaging: diagnostic accuracy in patients imaged within 6 hours of stroke symptom onset. *Radiology* 1999; 210:155-162.
12. Lin DD, Filippi CG, Steever AB, Zimmerman RD. Detection of intracranial hemorrhage: comparison between gradient-echo images and b(0) images obtained from diffusion-weighted echo-planar sequences. *AJNR Am J Neuroradiol* 2001; 22: 1275-1281.
13. Shimoda M, Hoshikawa K, Shiramizu H, et al. Clinical implications of subarachnoid clots detected by diffusion-weighted imaging in the acute stage of aneurysm rupture. *Neurol Med Chir (Tokyo)* 2010; 50: 192-199.

- Zimmerman RA, Bilaniuk LT. Intracranial hematomas: imaging by high-field MR. *Radiology* 1985;157:87-93.
14. Zimmerman RA, Bilaniuk LT. Intracranial hematomas: imaging by high-field MR. *Radiology* 1985;157:87-93.
 15. Bradley WG. MR appearance of hemorrhage in the brain. *Radiology* 1993;189:15-26.
 16. Fiebach JB, Schellinger PD, Gass A, et al. Stroke magnetic resonance imaging is accurate in hyperacute intracerebral hemorrhage. *Stroke* 2004;35:502-6.
 17. Hermier M, Nighoghossian N. Contribution of susceptibility-weighted imaging to acute stroke assessment. *Stroke* 2004;35: 1989-94.
 18. Attia S, El Khatib MG, Bilal M, Nassar H. Spontaneous intracerebral hematoma in young people: clinical and radiological magnetic resonance imaging features by diffusion-weighted images. *Egypt J Neurol Psych Neurosurg* 2007;44:561-76.
 19. Patel MR, Edelman RR, Warach S. Detection of hyperacute primary intraparenchymal hemorrhage by magnetic resonance imaging. *Stroke* 1996;27:2321-4.
 20. Atlas SW, Thulborn KR. MR detection of hyperacute parenchymal hemorrhage of the brain. *AJNR* 1998;19:1471-7.
 21. A Gonzalez RG, Schaefer P, Buonanno FS, et al. Diffusion-weighted MR imaging: diagnostic accuracy in patients imaged within 6 hours of stroke symptom onset. *Radiology* 1999;210: 155-62;
 22. Schellinger PD, Jansen O, Fiebach JB, Hacke W, Sartor K. A standardized MRI stroke protocol: comparison with CT in hyperacute intracerebral hemorrhage. *Stroke* 1999;30:765-8.
 23. Sunshine J, Tarr R, Lanzieri C, Landis D, Selman W, Lewin J. Hyperacute stroke: ultrafast MR imaging of triage patients prior to therapy. *Radiology* 1999;212:325-32.
 24. Linfante I, Llinas RH, Caplan LR, Warach S. MRI features of intracerebral hemorrhage within 2 hours of symptom onset. *Stroke* 1999;30:2263-7.
 25. Schellinger PD, Jansen O, Fiebach JB, Hacke W, Sartor K. A standardized MRI stroke protocol: comparison with CT in hyperacute intracerebral hemorrhage. *Stroke* 1999; 30: 765-768.
 26. Felber S, Auer A, Wolf C, et al. [MRI characteristics of spontaneous intracerebral hemorrhage]. [Article in German] *Radiologe* 1999; 39: 838-846.
 25. Wiesmann M, Mayer TE, Yousry I, Hamann GF, Brückmann H. Detection of hyperacute parenchymal hemorrhage of the brain using echo-planar T2*-weighted and diffusion-weighted MRI. *Eur Radiol* 2001; 11:849-853.
 27. 11:849-853.
 28. Atlas SW, DuBois P, Singer MB, Lu D. Diffusion measurements in intracranial hematomas: implications for MR imaging of acute stroke. *Am J Neuroradiol* 2000;21:1190-4.
 29. Schaefer PW, Grant PE, Gonzalez RG. Diffusion-weighted MR imaging of the brain. *Radiology* 2000;217:331-45.
 30. Wiesmann M, Mayer TE, Yousry I, Hamann GF, Brückmann H. Detection of hyperacute parenchymal hemorrhage of the brain using echo-planar T2*-weighted and diffusion-weighted MRI. *Eur Radiol* 2001; 11: 849-853.
 31. Kang BK, Na DG, Ryoo JW, et al. Diffusion-weighted MR imaging of intracerebral hemorrhage. *Korean J Radiol* 2001; 2: 183-191
 32. Ebisu T, Tanaka C, Umeda M, et al. Hemorrhagic and nonhemorrhagic stroke: diagnosis with diffusion-weighted and T2-weighted echo-planar MR imaging. *Radiology* 1997; 203: 823-828.
 33. Gomori JM, Grossman RI, Goldberg HI, Zimmerman RA, Bilaniuk LT. Intracranial hematomas: imaging by high-field MR. *Radiology* 1985; 157: 87-93.
 34. Bradley WG Jr. MR appearance of hemorrhage in the brain. *Radiology* 1993; 189: 15-26.
 35. Brooks RA, Di Chiro G, Patronas N. MR imaging of cerebral hematomas at different field strengths: theory and applications. *J Comput Assist Tomogr* 1989; 13: 194-206.
 36. Lin DD, Filippi CG, Steever AB, Zimmerman RD. Detection of intracranial hemorrhage: comparison between gradient echo images and b(0) images obtained from diffusion-weighted echo-planar sequences. *AJNR Am J Neuroradiol* 2001;22:1275-81.
 37. Kidwell CS, Warach S. Acute ischemic cerebrovascular syndrome. *Stroke* 2003;34:2995-8.
 38. Gomori JM, Grossman RI, Goldberg HI, Zimmerman RA, Bilaniuk LT. Intracranial hematomas: imaging by high-field MR. *Radiology* 1985; 157: 87-93.
 39. Bradley WG Jr. MR appearance of hemorrhage in the brain. *Radiology* 1993; 189: 15-26.
 40. Ekholm S. Intracranial hemorrhages. *Rivista di Neuroradiologia* 1996; 9:17-21.
 41. Moritani T, Ekholm S, Westesson P. Editors, DW imaging of Brain, Springer Berlin Heidelberg New York Business. 2005; 80-81.
 42. Bradley WG Jr. MR appearance of hemorrhage in the brain. *Radiology* 1993; 189: 15-26.
 43. Brooks RA, Di Chiro G, Patronas N. MR imaging of cerebral hematomas at different field strengths: theory and applications. *J Comput Assist Tomogr* 1989; 13: 194-206.
 44. Ekholm S. Intracranial hemorrhages. *Rivista di Neuroradiologia* 1996; 9:17-21.
 45. Gomori JM, Grossman RI, Goldberg HI, Zimmerman RA, Bilaniuk LT. Intracranial hematomas: imaging by high-field MR. *Radiology* 1985;157:87-93.
 46. Bradley WG. MR appearance of hemorrhage in the brain. *Radiology* 1993;189:15-26